Proceedings of the 28th IEEE
EMBS Annual International Conference
New York City, USA, Aug 30-Sept 3, 2006



# Statistical Bilateral Asymmetry Measurement in Brain Images

Xin Liu, R.Todd Ogden, Celina Imielinska, Andrew Laine
E. Sander Connolly, Anthony L. D'Ambrosio

*Abstract*—**We present an improvement of an automated generic methodology for symmetry identification, asymmetry quantification, and segmentation of brain pathologies, utilizing the inherent bi-fold mirror symmetry in brain imagery. In the pipeline of operations starting with detection of the symmetry axis, hemisphere-wise cross registration, statistical correlation and quantification of asymmetries, we segment a target brain pathology. The detection of pathological difference left to right in brain imagery is complicated by normal variations as well as geometric misalignment in anatomical structures between two hemispheres. Introducing hemisphere-wise registration and spatial correlation makes our approach perform robustly in the presence of normal asymmetries and systematic artifacts such as bias field and acquisition noise.**

## I. INTRODUCTION

Medical image segmentation, a process of identifying and delineating anatomical structures and other objects in medical images, still largely remains an open problem, in spite of several decades of research utilizing major imaging modalities [1]. Many brain segmentation approaches have evolved from low level image operations such as thresholding, edge detection, mathematical morphology [10], to more sophisticated image processing methods such as statistical classification[11][12], active contours[22], neural networks[4], fuzzy connectedness [23], level sets[28] and hybrid segmentation methods [24]. However, clinical applications suggest that to successfully differentiate between organ and tumor tissue, image information alone is often insufficient [6]. For example, if a tumor shows insufficient contrast against healthy brain tissue, active contour classification requires the selection of seeds to initialize segmentation, hence the method is not fully automated. Other statistical classification methods are also limited due to overlapping intensity distributions of healthy tissue, tumor, and surrounding edema. In the digital anatomical atlas –based segmentation [13] prior knowledge about normal brain anatomy is used, including the size, shape and location of anatomical structures. However, the shape and other characteristics of tumors and other brain pathologies are highly variable, thus representing prior knowledge about brain pathologies is hard to obtain.

In this paper, we propose an improvement of an automated generic method for identification, delineation and segmentation of the brain pathology by evaluating differences between opposing sides of the brain described in our prior work [25,26]. Inspired by atlas based methods, we replace the need for a generic digital atlas with the patient-specific brain template using healthy side of the brain as the prior model. Because normal brains exhibit high level of bi-fold mirror symmetry that is partially absent under pathological conditions. e.g tumor, stroke, bleed. We therefore utilize the inherent left-right symmetry to guide classification of human brain pathologies by cross-registration between opposing hemispheres and statistically enhancing the differences in a higher dimensional feature space.

Statistical tests operating on the paired windows are applied to identify seeds points in the pixels exhibiting statistically sufficient bilateral asymmetry. Hemisphere-wise registration has been adopted so as to eliminate the normal asymmetries as well as geometrical misalignments. Since we can't assume independent samples within two paired windows, intra-window and inter-window spatial correlation has been performed by computing the covariance modeled by correlogram [18-20]. The identified statistical difference has marked the seeds from where local adaptive region growing is performed with the stopping criteria predefined based on the intensities of the original images.

The paper is organized as follows. In section 2, we describe our algorithm in details and the results are discussed in section 3, where we demonstrate capabilities of our method on MR DWI (Diffusion-Weighted Images),a common MR technique that is used together with ADC (Apparent Diffusion Coefficient) map in the diagnosis of acute infarcts [25]. Finally, we present conclusions of our work and point out future directions in section 4.

## II. METHODS

In the pipeline of operations starting with detection of the symmetry axis, hemisphere-wise cross registration, statistical correlation and quantification of asymmetries, we segment the target brain pathology.

### *A. Identification of Symmetry Axis*

Various approaches for detecting, analyzing, measuring

Xin Liu is with Department of Biomedical Informatics, Columbia University. New York, NY 10032.USA; phone: 212-342-1632; fax: 212-342-1647; e-mail: xl2104@columbia.edu.

R. Todd Ogden , is with Biostatistics Department, Columbia University, New York, NY 10032.USA; email: ogden@neuron.cpmc.columbia.edu

Celina Imielinska, is with Department of Biomedical Informatics, Columbia University. New York, NY 10032.USA; email: ci42@columbia.edu.

Andrew Laine, is with Department of Biomedical Engineering, Columbia University . New York, NY10027 USA; Email: laine@columbia.edu

E. Sander Connolly, is with Neurosurgery Department, Columbia University, New York, NY 10032.USA; email: esc5@columbia.edu.

Anthony L. D'Ambrosio is with Neurosurgery Department, Columbia University, New York, NY 10032.USA; email ad504@columbia.edu.

and applying 2D symmetry in image analysis have been suggested [7, 8, 9]. In our early work [2, 3], an algorithm for detecting the symmetry axes of a 2D planar shape was presented.We map from an image $I(x,y)$ to $r$-$\theta$ polar space, which will give rise to an image $I(r,\theta)$ where the origin (0,0) in polar coordinates(see Fig.1b) corresponds to the centroid in the Cartesian coordinates (see Fig.1a)

For an object with a well-defined boundary, there are lines extending from the centroid $(\bar{x},\bar{y})$ with direction $\theta$ and length $r(\theta)$. In polar representation, to determine a two fold mirror symmetric axis we seek the $\varphi$ values that minimize the distance between two adjacent window of size $\pi$.

$$d_{\phi}^{p}(Right,Left)=\sqrt[p]{\int_{\theta=0}^{\pi}\left|r(\varphi+\theta)-r(\varphi-\theta)\right|^{p}d\theta}$$

Specifically, for $p$=1,

$$d_{\phi}^{1}(Right,Left)=\int_{\theta=0}^{\pi}\left|r(\varphi+\theta)-r(\varphi-\theta)\right|d\theta$$

with the best symmetry axis being

$$\varphi_{\tau}=\arg\min d_{\phi}^{1}(Right,Left)\cdot$$

The resulting $\varphi$ minimizes the absolute distance between two adjacent windows of size $\pi$. Therefore, the problem turns into identifying the global minimum of symmetry measure $d$ in the polar space. This can be implemented by comparing the left-half and right-half of a sliding window across the entire $r$-$\theta$ space, as shown in Fig 1.

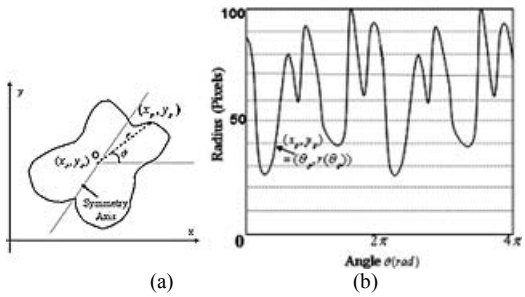


(a) (b)

Fig. 1. (a) The axis of symmetry in an almost symmetrical object. Each point has been re-parameterized by its radius $r$ and the angle $\theta$. (b) In $r$-$\theta$ polar space, we seek the global minimum of the absolute distance between two adjacent windows of size $\pi$.

### *B. Non-rigid registration between two hemispheres*

The normal asymmetries between hemispheres can be statistically significant. Misalignment in geometry and variance in intensities, as shown in Fig.2(a), can complicate procedures to precisely segment pathologies. If there appears a dramatic normal variation between two hemispheres, it is highly likely that the method will pick up unwanted artifacts together with pathological asymmetries. In order to eliminate these artifacts, we conduct non-rigid registration between the two hemispheres as a preprocessing step such that points in the first half of the brain are mapped to their counterparts by geometric affine transformations.

Since we want to address both the intensity variance and geometrical misalignments between two hemispheres, we choose an intensity based approach so as to avoid the various pitfalls involved in feature selection. Geometrically, we adopt the algorithm to model the transformation with a local affine model and a global smoothness constraint. This allows us to capture non-linear distortions in both geometry and intensity. This entire procedure is built upon a differential framework, and the standard MSE error metric on intensity values is employed [21]. We let one scan be represented as $X(r,c)$, $r \in \{1,2,..N_Y\}$, $c \in \{1,2,..N_X\}$, where $N_X$, $N_Y$ are the $x$, $y$ dimensions of each scan. Since we have already re-aligned the brain along the symmetry axis $c_{sym}= N_X/2$, we split the image into two halves according to the symmetry axis. To create pairs of image elements the right or left set of pixels is flipped along the symmetry axis, therefore we have obtained the source $X_L$ and target $X_R$ halves of the brain, denoted in Fig.2 (a). The geometric transformation is followed to register all points in $X_L$ to corresponding points in $X_R$. The warped source $X_L'$, as shown in Fig.2(b), is more geometrically comparable with the target.

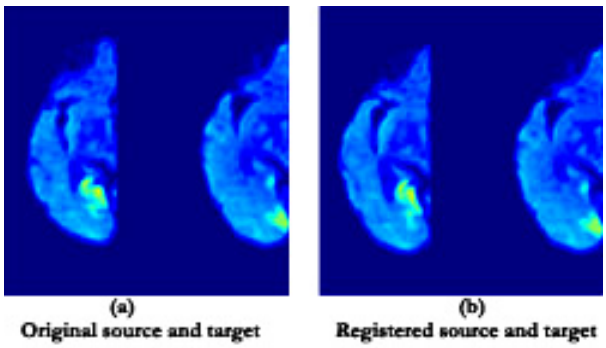


Fig. 2. A non-rigid registration is accomplished by geometric transformation demonstrated on a DWI image. (a) Original source and target halves of the brain. After the geometric mapping from the source half to the target, the registered source and target halves are shown in (b).

### *C. Modeling spatial correlation*

We consider all the artifacts other than pathological asymmetries as noise. We model the spatial correlation (see Fig.3.) using an isotropic exponential model with a "nugget" effect $C(R) = c_e\, exp(-R/a_e) + c_0\, 1_{\{R=0\}}$, where $R$ is the distance between pixels and $c_0$, $c_a$, and $a_e$ are model parameters to be estimated [25]. The model is fit using standard least squares methodology [20] to the differenced image (left hemisphere image subtracted from flipped right hemisphere image) to eliminate as much anatomical detail as possible, and the fitted covariance function is divided by two when applied to the original image.

### *D. Statistical Tests*

The neighborhood of a pixel is defined as a set of offsets both in columns and rows from this pixel, as shown below. The neighborhood is used to create the vicinity of the point $(r,c)$ of image $X$:

$$S_N : X(r,c)=\{X(r,c):(r+\Delta r,c+\Delta c),(\Delta r,\Delta c)\in N\}$$

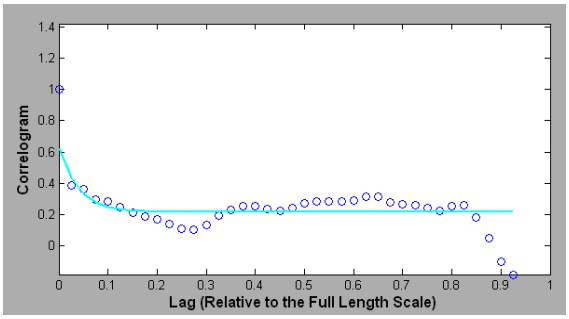


Fig. 3 Correlogram computed from brain data to model the spatial correlation. X coordinate is the relative distance of each pairs of pixels, and y coordinate is the estimated covariance that is a function of distance R. Coefficients can be estimated from least square fitting (the cyan curve)

We define the statistical tests sampling unit to be the square-shaped neighborhood, with window size $w=\Delta r=\Delta c$. Therefore two windows $(a_{i,j})_{w\times w}$, $(b_{i,j})_{w\times w}$, from the hemisphere $X_L'$ (the warped half brain through non-rigid registration) and from the hemisphere $X_R$ form two sample units, $1 \le i \le w, 1 \le j \le w$ . We slide each of the two windows across the entire half of the image and conduct statistical analysis sequentially (see Fig.4.).

The test statistic to be applied to each location (equivalently, to each window pair) is the mean difference between the pixels in the left window and the pixels in the right window, normalized according to the modeled covariance structure to have an approximate standard normal distribution in the absence of pathology. The variance of each window pair can be shown to be equal to

$$\delta = 2J^T \Sigma J - 2J^T \Sigma_r J ,$$

where J represents a vector of all ones, $\Sigma$ is the variance-covariance matrix of the pixels in each window, and $\Sigma_r$ is the covariance matrix for the vector of pixels in the right window and those in the left window.

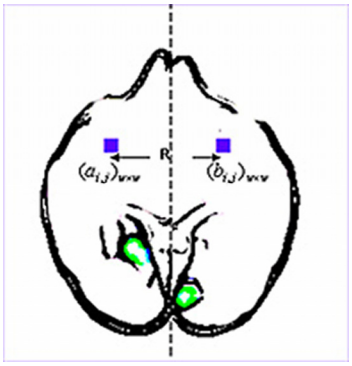


Fig. 4 Statistical correlation and significance test are performed based on two paired windows as our sample units. The covariance of a given two elements within those two windows is modeled by correlogram that is a function of distance R.

These are computed based on the fitted model for the spatial correlation (Fig.3.). Note that, due to the assumed isotropy of the covariance structure, $\Sigma$ does not depend on location and $\Sigma_r$ depends only on the distance from the window to the axis of symmetry. Thus this quantity needs to be computed for each possible distance. The test statistic is the mean difference between pixels from two windows divided by the square root of the variance and this can be compared with the standard normal quartiles to judge significance.

$$u = \frac{\sum_{i=1}^{w}\sum_{j=1}^{w}\left|(a_{i,j} - b_{i,j})\right| \ / w^2}{\sqrt{\delta_{ab}}}$$

$\delta_{ab}$ is the variance between each paired windows.

*E. Adaptive Region Growing*

In stroke DWI (diffusion weighted image), it is known that stroke intensities are significantly higher than the normal tissue [25]. We filter the statistical differences $u$ applying a secondary threshold based on intensities of the original image. This gives rise to the seeds map, see Fig.5. (c). Local adaptive region growing is performed starting from the seeds, and a threshold value, 1.96 standard deviations of the mean value of the seeds grown, is used to test if the candidate is sufficiently similar to the seeds; This corresponds to a finding of a 5% chance that a sampled case will lie outside 1.96 standard deviations of the mean. Therefore, the value of each candidate pixel is compared with the average intensity of the seed region grown. This step is iterated until convergence. If the pixel is 8-way connected to one or more seed values, then the pixel may be considered a member of one or more regions. A sample of the final segmentation results is shown in Fig.5.(d).

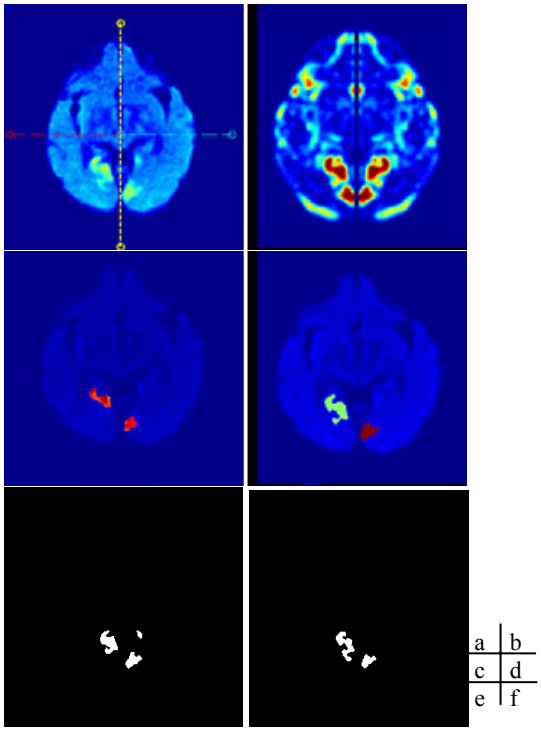


Fig. 5. The proposed methodology first identifies the symmetry axis of any input data(a), then the spatial correlation and the test statistic yield the image (b). Seeds(c) have been extracted from statistical tests and region growing makes the segmentation of the pathological asymmetries complete(d). (e),(f) are the ground truth delineated by expert 1 and expert 2. Full description of generating ground truth can be found in our early work [25].

## III. RESULTS

We illustrate below our technique on DWI images. Common MR imaging techniques such as DWI and ADC maps are used routinely in the diagnosis of acute stroke. We can delineate regions of acute stroke on DWI and ADC

maps, and these two together can best verify the presence of absence of acute infarcts. In this paper we demonstrate on an example of a DWI image how a brain pathology can be automatically delineated by our improved segmentation method as shown in Fig. 5. We previously conducted accuracy assessment of an earlier version of our symmetry-based segmentation, [26], of DWI stroke region [25], where a surrogate of ground truth was generated by two independent experts. In Fig. 5, we show that the new method improves our previous results computed for the same patient data in [25], as shown in the tables below. We used accuracy evaluation parameters from [27]. As part of the accuracy assessment, three different values were obtained: 1) true positive volume fraction (TPVF) is the fraction of the total amount of tissue in the ground truth which overlaps with the experimental method delineation, 2) false positive volume fraction (FPVF) is the fraction of tissue falsely identified and 3) false negative volume fraction (FNVF) is the fraction of tissue that was missed. The accuracy measurement values are shown in Tables 1,2.

The older version of the method captured both pathological asymmetry as well as the artifacts caused by the non-uniformity of the intensities, also known as bias field. The hemisphere-wise cross registration and spatial correlation adjustments makes our approach perform more robustly in the presence of normal asymmetries and systematic artifacts such as bias field, see Fig. 6 (c).

TABLE 1.
ACCURACY MEASUREMENTS FOR EXPERT1 GROUND TRUTH (GT) AS COMPARED WITH OUR SEGMENTATION ALGORITHM

| Expert1 GT Area | Seg. Area | Area Diff. (%) | FNVF | FPVF | TPVF |
|---|---|---|---|---|---|
| 460 | 444 | 3.47 | 0.158 | 0.123 | 0.841 |

TABLE 2.
ACCURACY MEASUREMENTS FOR EXPERT2 GROUND TRUTH (GT) AS COMPARED WITH THE RDM DWI SEGMENTATION ALGORITHM.

| Expert2 GT Area | Seg. Area | Area Diff. (%) | FNVF | FPVF | TPVF |
|---|---|---|---|---|---|
| 452 | 444 | 3.69 | 0.172 | 0.146 | 0.823 |

(a) (b) (c)

Fig.6. Segmentation of stroke region in a DWI image. (a) original input image looks asymmetrical apart from the infarct region, because of the bias field (b) segmentation result generalized by previous work[25], using non-parametric statistical test (c) segmentation result using current approach, the outliner caused by the bias field has been removed

## IV. CONCLUSION

In this paper we present a generic method for computing axis of symmetry and quantification of asymmetries in brain imagery. This approach consists of: 1) identifying the axis of symmetry; 2) cross registration between hemispheres; 3) statistical correlation and computation of differences 4) segmentation of targeted brain pathologies. The preliminary results have shown that this approach has promise to achieve high precision and full automation, that is lacking in most segmentation methods, in segmenting brain lesions through symmetry analysis. The future work involves extending this method from 2D scans to 3D volumes so that the global volumetric pathological asymmetries can be captured and classified.

## ACKNOWLEGMENT

The funding source of this project comes from Department of Neurosurgery, Columbia University.

## REFERENCES

[1] D. Pham, C. Xu and J. Prince, “Current Methods in Medical Image Segmentation”, Annual Review Biomedical Engineering, 2:315-337, 2000.

[2] X. Liu, C. Imielinska, J. Rosiene, at al.”A novel quantification method for determining previously undetected MR perfusion changes in patients with cognitive deficits following carotid endarterectomy”, *SPIE2005 Medical Imaging*.

[3] Imielinska C., X. Liu, M. Sughrue, E. Hagiwara, E.S. Connolly, A. D’Ambrosio, “Objective Quantification of Perfusion-Weighted Computer Tomography in the Setting of Acute Aneurysmal Subarachnoid Hemorrhage”, *Computer Assisted Radiology and Surgery*, pp. 34-43, June 2004

[4] C. Imielinska, X. Liu, J. Rosiene, at al, “Towards Objective Quantification of Perfusion- Weighted Computed Tomography in the Setting of Subarachnoid Hemorrhage: Quantifica tion of Symmetry and Automated Delineation of Vascular Territories”. *Academic Radiology*.2005, 12:874-887.

[5] C.E. Metz, “ROC methodology in radiologic imaging”, *Invest. Radiology,* Vol. 21,pp. 720-733, 1986.

[6] Michael R. Kaus, Simon K. Warfield, Arya Nabavi, Peter M. Black, Ferenc A. Jolesz, and Ron Kikinis Automated Segmentation of MR Images of Brain Tumors Radiology 2001; 218: 586.

[7] D.Reisfeld, H.Wolfson and Y.Yeshurun. “Context Free Attentional operators: the generalized symmetry transform”. IJCV, vol.14,pp.119-130,1995.

[8] Gofman, Y.; Kiryati, N.; “Detecting symmetry in grey level images: the global optimization approach” Pattern Recognition, 1996., Proceedings of the 13th International Conference on , Volume: 1 , 25-29 Aug. 1996

[9] J.Bigun, “Recognition of Local Symmetries in Gray Value Images by Harmonic Functions”, Proc. 9th ICPR, pp.345-347, Rome, 1988.

[10] J. Serra. Image Analysis and Mathematical Morphology. Academic Press, 1982.

[11] L.P. Clarke, R.P. Velthuizen, S. Phuphanich, J.D. Schellenberg, J.A. Arrington, and M. Silbinger. MRI: Stability of Three Supervised Segmentation Techniques. Magnetic Resonance Imaging, 11(1):95-106, 1993.

[12] G. Gerig, J. Martin, R. Kikinis, O. Kübler, M. Shenton, and F.A. Jolesz. Unsupervised Tissue Type Segmentation of 3D dual-echo MR Head Data. Image and Vision Computing, 10(6):349-360, 1992. IPMI 1991 Special Issue

[13] R. Kikinis, M.E. Shenton, D.V. Iosifescu, R.W. McCarley, P. Saiviroonporn, H.H. Hokama, A. Robatino, D. Metcalf, C.G. Wible, C.M. Portas, R. Donnino, and F.A. Jolesz. A Digital Brain Atlas for Surgical Planning, Model Driven Segmentation and Teaching. IEEE Transactions on Visualization and Computer Graphics, 2(3):232-241, 1996

[14] B. Klaus, P. Horn. “Robot Vision”, MIT press, pp. 48-58.

[15] J. Rosiene, X. Liu, C. Imielinska, "Ray casting approach for boundary extraction and Fourier shape descriptor characterization", SPIE Electronic Imaging, Feb. 2005

[16] Denman, K.L. and H.J. Freeland, 1985. Correlation Scales, Objective Mapping and a Statistical Test of Geostrophy over the Continental Shelf. J. Mar. Res., 43: 517-539.

[17] Deutsch, C. V and A. G. Journel, 1992. *GSLIB: Geostatistical Software Library and User's Guide*. Oxford University Press, Oxford, 340 p.

[18] Journel, A.G. and C.J. Huijbregts, 1992. *Mining Geostatistics*. Academic Press, New York, 600 p.
[19] Marcotte, D. 1991. Cokrigeage with MATLAB. Computers & Geosciences. 17(9): 1265-1280.
[20] Dezhang Chu, "Kriging Software for MATLAB 5.2" http://globec.whoi.edu/globec-dir/reports/siworkshop1998/report_chu_kriging.html
[21] S. Periaswamy, J.B. Weaver,D.M. Healy Jr., D. Rockmore, P.J. Kostelec, and H. Farid. "Differential Affine Motion Estimation for Medical Image Registration" *Proceedings of the SPIE*4119, pp.1066-1075,2000.http://www.cs.dartmouth.edu/~farid/research/registration.html
[22] T. McInnerney and D. Terzopoulos. Deformable Models in Medical Image Analysis: A Survey. Medical Image Analysis, 1(2):91-108, 1996.
[23] J. Udupa and S. Samarasekera, "Fuzzy Connectedness and Object Definition: Theory, Algorithms, and Applications in Image Segmentation." Graphical Models and Image Processing, vol. 58 (3), pp. 246-261, 1996.
[24] C. Imielinska ., J. Udupa, D. Metaxas, Y. Jin, E. Angelini, T. Chen, Y Zhuge, "Hybrid Segmentation Methods", book chapter in "Insight into Images: Principles and Practice for Segmentation, Registration, and Image Analysis", edited by T. Yoo, A.K. Peters, March 2004
[25] P.K. Tulipano, W. Millar, C. Imielińska, , X. Liu, J. Rosiene, M. Sughrue, A. D'Ambrosio, "Quantification of Diffusion Weighted Images (DWI) and Apparent Diffusion Coefficiant Maps (ADC) in Detection of Acute Stroke", SPIE Medical Imaging 2006.
[26] X. Liu, C. Imielińska**,** , J. Rosiene, M. Sughrue, E.S. Connolly, A.L. D'Ambrosio, "Enhanced Technique for Asymmetry Quantification in Brain Imagery", *SPIE Medical Imaging 2006.*
[27] Udupa JK LV, Schmidt H, Imielinska C, Saha PK, Grevera GJ, Zhuge Y, Currie LM, Molholt P, Jin Y. . Methodology for evaluating image-segmentation algorithms. SPIE Conference on Medical Imaging. 2002;4684:266-77.
[28] Baillard C, Hellier P, Barillot C. "Segmentation of brain 3D MR images using level sets and dense registration." Med Image Anal. 2001 Sep;5(3):185-94.